Flow of pH-responsive microcapsules in porous media

*Wei Jin Gun and Alexander F. Routh**

BP Institute for Multiphase Flow, Department of Chemical Engineering and Biotechnology, University of Cambridge, CB3 0EZ, United Kingdom.

Abstract

This article investigates the use micro-capsules, containing a gelling agent hydroxypropyl cellulose (HPC), to alter flow paths in porous media. The aim is to preferentially block-off high permeability regions, thereby diverting the flow into adjacent un-swept low permeability regions. Micro-capsules with 2 – 7 μm in diameter, were made by polymer precipitation through solvent evaporation usingpoly(4-vinyl pyridine) (PVP) as the shell material. A customized flow tank was constructed to facilitate porous media flow and both single and dual permeability experiments were conducted. Even without gelling agent, the micro-capsules gradually blocked the pore throats of the glass beads network. Following acidification a drop in permeability was observed. This was because swelling of the PVP shell constricted the pore throats. The permeability drop was observed to be more significant for low permeability regions. Flowing micro-capsules through the tank with two permeability regions in parallel, allowed the high permeability region to be selectively blocked.

Keywords: Encapsulation; Enhanced oil recovery; Triggered release; Porous media

1.Introduction

Micro-capsules are micron-sized particles. They comprise a shell, encapsulating an active ingredient, in the core. The shell acts as a barrier between the active ingredient and the potentially harsh external environments, which can be imposed on the micro-capsules. Such harsh environments can be mechanical, thermal or chemical depending on the situation. There are numerous examples in the pharmaceutical industry where encapsulation would be beneficial. For example, if biological materials such as enzymes, which are susceptible to denaturation, are encapsulated their biological activity can be retained (Keen et al., 2012; Nasseau et al., 2001). Other examples include the encapsulation of astaxanthin, a food supplement, which showed minimal heat degradation compared to free astaxanthin(Tachaprutinun et al., 2009). Encapsulation is also important in the digital display industry, for example by increasing the lifetime of organic light-emitting diodes, by preventing moisture and oxygen diffusion into the display area (Chwang et al., 2003; Seo et al., 2013).

Within the oil industry, no journal articles concerning the use of micro-capsules for enhanced oil recovery could be found. This is likely due to the lack of an appropriate time response, cost, the required sub-micronparticle size for low porosity reservoirs, and harsh reservoir conditions with high salinities and temperatures. So far, only patents have been found studying this area (Bertkau et al., 2012; Montanaro, 2012).

During secondary oil recovery, water is pumped into an oil field, via an injector, to maintain reservoir pressure and to sweep more oil towards the producer. Typically, the injected water will propagate via the path of highest permeabilityand can leave large regions of the oil field un-swept. The idea behind this work is to flow micro-capsules, containinga gelling polymer into a porous medium before a stimulus/trigger is applied to release the payload. The released polymer then forms a gelled network, causing a marked drop in permeability, or better still, completely blocking off that particular swept region. The following water is then diverted into the adjacent un-swept regions therebymobilising the oil trapped in these regions.

Flow of micro-capsules in porous media, for temperature triggered micro-capsules, was investigated in a previous paper (Gun and Routh, 2013b). In this article, pH is pursued as a release mechanism, by using micro-capsules with a poly(4-vinyl pyridine) (PVP) shell. The synthesis and characterisation of these micro-capsules was reported previously (Gun and Routh, 2013a) and release of the core material was demonstratedwhen exposed to acidic environments, because of dissolution of the polymeric shell.

The use of pH as the release trigger is fundamentally different to temperature. The temperature profile within a porous medium can be externally set, but for pH release, one needs to flow an acidic solution into the bed. Acid injection into reservoirs is an area that is extensively researched. One purpose of acid injection is to dissolve carbonate minerals, opening up the rock for fluid flow. These highly conductive channels can then form a comprehensive network allowing trapped oil to be swept out. If the acid was pumped at a high pressure, rock formations within the reservoirs can also be fractured, allowing the acid to etch into the fractures, forming

more channels (Samuel and Sengul, 2003). This study uses acid to trigger microcapsule release and consequently is likely to be relevant to sandstone reservoirs.

Another possible application for these micro-capsules would be in the field of chromatography. Itwould be of interest to conduct experiments with a distributed system of permeabilities,rather than two distinctive permeability layers, as reported in this paper. This would be relevant to preparative chromatography, where heterogeneity in the porosity of the chromatographic medium gives rise to greater dispersion of eluents. Permeability patterns in porous media strongly influence the flow as shown through flow visualisation work (Tchelpi et al., 1993). Using micro-capsules, one would decrease the permeability spread in the chromatographic column, allowing sharper peaks in the chromatogram, resulting in a higher separation purity.

In this paper, we report the use of pH sensitive micro-capsules to release hydroxypropyl cellulose (HPC) into a bead pack, upon addition of acid. The aim of the paper is to demonstrate that flow paths within a porous medium can be altered using micro-capsules.

2. Materials and Method

2.1 Microcapsule formation and release profile

Micro-capsules that are pH-responsive were made with a PVP (M_w~160,000, Sigma-Aldrich) shell and an aqueous core containing HPC (M_w 370,000, Sigma-Aldrich). They were made using a polymer precipitation method, which has been discussed previously (Gun and Routh, 2013a). These micro-capsules displayed an enhanced release when exposed to aqueous solutions below pH 3.5. The concentration of HPC in the core was 10 wt% in water and the capsules were

determined from SEM images to be 2-7 μm in diameter. SEM images of the particles are shown in Figure 1.

2.2 Tank Set-up

To assemble, the tank was initially flooded with deionised water 18.2 MΩ cm (Purelab Ultra from ELGA process water) before pouring 3 mm diameter glass beads up to a height of 40 mm. A photo of the tank is shown in Figure 2 with a schematic shown in Figure 3. The main reason for flooding the tank with deionised water was to prevent trapped air pockets within the pack. This was frequently observed for glass beads less than 1 mm diameter and required the glass beads to be stirred vigorously to remove. The tank was then filled with 0.5 mm and 1.0 mm diameter glass beads on the two sides, separated with an impermeable Styrofoam partition, until they reached a height of 160 mm. A 40 mm layer of water was placed above the 0.5 mm and 1.0 mm beads to provide a constant pressure head. The pressure gradient, ΔP across the porous pack could be adjusted by changing the height of the outlet pipe. At the end of the outlet pipe was a mass balance, which recorded the outflow every second. By varying ΔP, we measured the change in actual flow rate. From the data-log, a graph of fluid mass against time was plotted and the gradient corresponded to the flow rate, Q. Figure 4a shows the data one obtains.To ensure continual flow, the tank was never allowed to drain of water.

To predict the flow rate, the porous medium was made of various glass beads combinations in parallel and series as shown in Figure 4b. Hence, the total tank permeability, K_T can be calculated as a function of lengths L_1, L_2, L_T and individual permeability layers K_1, K_2 and K_3.

For two regions in parallel with a third in series, it is trivial to show that the total permeability, K_T, is given by

$$K_T = \frac{L_T K_3}{L_2}\left[\frac{K_1 + K_2}{\frac{2K_3}{L_2/L_1} + K_1 + K_2}\right] \quad (1)$$

2.2.1 Pipe Losses

The scale of the tank is much larger than that used for the temperature-responsive micro-capsules (Gun and Routh, 2013b). With the tank having dimensions of 250 mm × 145 mm × 10 mm, the flow rate is larger through the pipe outlets. Hence, the pressure losses in the pipes have to be accounted for, before calculating the permeability changes in the tank. The pressure drop in a pipe, due to friction, is given by (Sinnott, 2005),

$$\Delta P_f = 8f\frac{L_p}{d_i}\frac{\rho u^2}{2}, \quad (2)$$

where ΔP_f is the pressure loss (kg m^{-1} s^{-2}), f is the friction factor, L_p is the pipe length (m), d_i is the pipe internal diameter (m), ρ is the fluid density (kg m^{-3}) and u is the fluid velocity (m s^{-1}).

Darcy flow is defined by:

$$Q = \frac{KA\,\Delta P}{\mu L}, \quad (3)$$

where Q is the flow rate (m^3 s^{-1}), A is the flow area (m^2), ΔP is the pressure difference (kg m^{-1} s^{-2}), μ is the fluid viscosity (kg m^{-1} s^{-1}) and L is the length of the porous pack (m).

The friction factor is dependent on the Reynolds number, $Re = {\rho u d_i}/{\mu}$ and pipe roughness. A correlation between pipe friction, Reynolds number and pipe roughness is readily available from Moody diagrams(Moody, 1944).

To avoid the problem of pressure losses across pipes, the pressure drop across the tank, ΔP was decreased by reducing the output flow rate, Q, as given in Equation (3). A lower fluid velocity, u gave a lower pressure loss, ΔP_f as shown in Equation (2). Comparisons were then made between the measured flow rate and that predicted using equation 1, for zero pipe losses. The pipe losses scale with the velocity squared whereas Darcy flow has a linear relation between pressure drop and flow rate. Hence, as the flow rate is reduced, the pipe losses become progressively less relevant.

2.3 Single permeability experiments

Before conducting dual permeability experiments, investigations on a single permeability layer were carried out. This was achieved by using only one side of the tank shown in Figure 2.

To assemble the experiment, the tank was flooded with water, before glass beads of diameter 1 mm were poured into the tank while stirring with a rod to remove any trapped air bubbles. Once the micro-capsulesreached a height of 200 mm, the remaining 40 mm height was filled with deionised water. For a typical experiment, the initial permeability of the tank was measured by flowing deionised water for a few pore volumes. This was then followed with one pore volume of a dispersion containing 10 vol% PVP shell micro-capsules (with HPC in the core) and then a further three pore volumes of deionised water. This step was repeated to determine whether a

gradual decrease in permeability would be seen from the accumulation of multiple micro-capsule flushes. After this, three pore volumes of acid were added to release the HPC in the core. Throughout the entire experiment, the fluid output was recorded using a mass balance. The experiment was also repeated for micro-capsules with only water in the core and for glass beads of diameter 0.5 mm, to determine the effect of initial permeability.

To calculate the total permeability, the gradient of the fluid mass against time curve was calculated to determine the fluid flow rate Q. Using Darcy's Law, Equation (3), the total permeability K_T was calculated. To determine the pore volume, the tank was filled with deionised water followed by red dye (bright red powder by PREEMA dissolved in deionised water). While flowing the dye, the volume of water displaced was measured. This displaced volume corresponded to one pore volume of the tank.

2.4 Dual permeability experiments

For experiments with two permeability layers in parallel, a metal mesh was introduced in the middle of the high permeability layer as shown in Figure 2. The purpose of this metal mesh is to support a piece of filter paper to trap the micro-capsules, hence increasing the local concentration of HPC released from the cores of the PVP micro-capsules. The filter paper used was Durapore Membrane Filters, manufactured by Milipore, with a pore size of 0.65 μm. The addition of this filter paper changed the permeability of the high permeability zone by less than 8%. To enable the filter paper to be anchored securely on the metal mesh, the borders of the filter paper were sandwiched between laminations and cut into the exact size of the metal mesh support.

After assembly, the tank was flowed with deionised water and dye a couple of times to determine the initial tank permeability. 100 mL of the 10 vol% PVP shell micro-capsules, with HPC in the core at 10 wt%, was flowed into the high permeability layer only. This was then followed with two to three pore volumes of deionised water in both regions of the tank. Once again, 200 mL of the micro-capsule dispersion was flowed into the high permeability layer. Again, two to three pore volumes of water were flushed through the entirety of the pack. Pictures were then taken with red dye indicating the flow front progress to compare the relative flow changes in the high and low permeability layers. Subsequently, two pore volumes of pH 2 hydrochloric acid was added to release the HPC from the trapped micro-capsules by swelling the PVP shell, releasing the HPC core. After acid flow, the flow fronts were tracked with dye again. Whenever red dye was used, to track the relative flow fronts, pictures were taken every 5 seconds.

In a final set of experiments, the micro-capsules were flowed through both layers simultaneously.

3. Results and Discussion

3.1. Pressure losses across pipes

Table 1 shows the results of the comparison between the measured and predicted flow rates. As expected, higher pressure differences resulted in higher volumetric flow rates and larger deviations from the prediction. This is because of pressure losses in the pipes. Therefore, it was decided to use a pressure difference of 402 Pa, which gave a low error. It should be noted that the predicted flowrates neglected the thickness of the impermeable partition, between the low

and high permeability layer. If this were to be accounted for, the predicted flow rate would be slightly lower, resulting in an even lower percentage error.

3.2 Single permeability experiments

The results for permeability against pore volumes of added micro-capsules show similar patterns irrespective of the bead size. The initial permeability drops to its lowest point during the initial micro-capsule injection as the micro-capsules flow through the porous media, sticking to the glass beads, thus closing the pore throats. This has also been reported in our previous paper (Gun and Routh, 2013a) for similar experiments but with temperature-responsive micro-capsules with HPC in the core. With the initial pore throats of 39 μm (based on 0.5 mm diameter glass beads) and 78 μm (based on 1.0 mm diameter glass beads), the micro-capsules of sizes 2-7 μm should have no trouble passing through the porous medium(Avery and Ramsay, 1973; Ciftcioglu et al., 1988; Kruyer, 1958). However, a drop in permeability suggests an interaction between the micro-capsules and glass beads.

For the high permeability layer case with HPC in the core, as shown in Figure 5a, the permeability dropped to almost zero with the first pore volume of micro-capsules. After three pore volumes of deionised water, some of the micro-capsules remained within the pack and the permeability ratio did not return to its initial value. Subsequent micro-capsule and water flushes, denoted by ◊, revealed a quicker drop in permeability. The final permeability ratio after the second micro-capsule and water flushes was lower than after the first flush, presumably due to accumulation of micro-capsules in the bead pack which constricted the pore throats further. Interestingly, with the flow of pH 2.2 hydrochloric acid, a slight drop in permeability within the

first pore volume was noted before the permeability ratio reaches a plateau reading of about 0.4 by the second pore volume of acid. The increase in permeability on flowing acid could be due to the HPC being released from the core, and then getting flushed out with the acid. This non-sticking behaviour of HPC was also seen in the case using a low permeability (Figure 6a).

For the micro-capsules without HPC in the core, as shown in Figures 5b and 6b, the drop in permeability ratio is less, because of the absence of the thickening agent. Without HPC, we would expect no drop in permeability in acidic conditions and this is the case for the high permeability layer experiments, denoted by × in Figure 5b. This behaviour was not seen for the low permeability experiment. A drop in permeability in the first pore volume of acid flow, denoted by × in Figure 6b, was still encountered. This could possibly be caused by the swelling of the micro-capsule shells adhered onto the glass beads surface, constricting the pore throats of radius 39 microns in the first pore volume of acid before completely dissolving and being flushed out with the remaining pore volumes. This is sketched in Figure 7b. This pattern was not observed in the high permeability experiment as the pore throats are larger (78 microns) and the swelling did not significantly block the pore throats, as sketched in Figure 7a.

Because the HPCappeared to have been flushed out with the macroscopic flow, some sort of device was required to ensure the hydroxypropyl cellulose had a high enough concentration to block the pore throats. This was the reason for using the filter paper, to collect the micro-capsules and increase the local concentration of HPC,when released from the core. The HPC core concentration was limited to 10 wt% as higher concentrations were too solid to enable micro-capsule production.

3.3 Dual permeability experiments

With the incorporation of the filter paper on the metal mesh, it was hoped that the increased concentration of HPC would cause a significant drop in the high permeability zone. The dual permeability experiments reported in this section were performed in two different ways. The difference concerned the flowing of the micro-capsule dispersion into the tank. The experimental results in Figure 8, were obtained by selectively flowing the micro-capsules only into the high permeability layer, ignoring the lower permeability layer.The experimental results in Figure 10, were obtained by pouring the micro-capsule dispersion in the centre of the tank, to allow free flow into both layersand uniform spreading. It should be noted that the numbers in parentheses in the figure captions indicate the flow sequence for the experiments.

For the selective flow experiment, shown in Figure 8, the results demonstrate that there is an accumulative effect offlowing more micro-capsules into the high permeability layer. This is shown by the first flush, denoted by ×, and second flush, denoted by +, which showed a decrease in permeability ratio from a plateau value of about 0.5 to 0.4 by the end of the second micro-capsule flow. This tallies with the single permeability experiment in Figure 5 which showed a progressive drop in permeability after two successive treatments of micro-capsules and chase water. The drop in permeability is due to the accumulation of micro-capsules both in the porous media network and filter paper. It should be noted that the data for the micro-capsule flow for the micro-capsule and water experiments, numbered as (4) and (5) in the legend of Figure 8,only shows the water flow. The reason for this truncation is because micro-capsuleswere selectively flowed into the high permeability layer, hence it would not have been consistent to plot the

micro-capsule flow with pore volume, sincethe pore volume involves the entire void volume in all layers. It was noted that during the water flushes, the permeability gradually increases as trapped micro-capsules are flushed out from the system, revealing larger pore throats for fluid flow. It is interesting that the permeability slowly changes during dye flow, denoted by △ and ■. This indicates the possible rearrangement ofmicro-capsules even after flushing with three pore volumes of deionised water.

Flow front pictures, taken during dye flows, are shown in Figure 9. These reveal that the relative flow fronts were altered in a similar fashion to the temperature-responsive micro-capsules reported previously (Gun and Routh, 2013a). By comparing the flow front heights, aided by the drawn arrows in the pictures, the relative flow rate of the high and low permeability layers was calculated. Before micro-capsule flow, shown in Figure 9a, the flow front for the high permeability layer was 5 times faster than the low permeability layer. This value dropped to 2.4 after successive micro-capsule and water flushes. Here, micro-capsules were shown to block the high permeability layer. Even though the blocking was not complete, a significant amount of water was diverted into the low permeability layer.

For the experiment with non-selective micro-capsule flow, shown in Figure 10, a similar pattern was observed. The lowest permeability was observed at about two pore volumes, as opposed to the temperature-responsive micro-capsule which recorded the lowest permeability reading at one pore volume. This can be explained in terms of the water flushes for this experiments which only came after 200 mL of micro-capsules (roughly two pore volumes), compared to the one pore volume of micro-capsules in the temperature-responsive experiments. After these two pore

volumes of micro-capsules, denoted by +, the deionised water then gradually flushes the micro-capsules, as indicated by the permeability ratio which reached a plateau value of about 0.35. There is data scatter for the second micro-capsule and water flow experiment, denoted by•, because the outflow was extremely slow and the pressure difference had to be increased by adjusting the height of the output flow pipe. After about five pore volumes, the pressure difference was adjusted back to 402 Pa. The permeability ratio reached a plateau value of about 0.4. We only report the data collected when the pressure difference was 402 Pa.

With acid flow, denoted by♦, an initial drop in permeability was seen up to about one pore volume before the permeability started to rise and the permeability ratio levelled off at about 0.5. This dropping behaviour, up to one pore volume, has been observed in the temperature-responsive micro-capsules containing HPC as well. This could suggest the swelling of the PVP shell, releasing the HPC within the core. The swelling of the micro-capsules would constrict the pore throats of the low permeability layer substantially, as seen in the single permeability experiments, causing a drop in permeability. This swelling will not affect the high permeability layer as much because the pore throats are larger. Nevertheless, the release of HPC would contribute to the decrease in permeability in both layers but this effect did not last a significant time, as the permeability began to increase again due to the HPC being flushed out from the system.

Flow front experiments with red dye are shown in Figure 11. Before any microcapsule treatment the high permeability layer is 4.5 times faster flowing than the low permeability layer. After one treatment of micro-capsules and a flushing of 10 pore volumes of water the high permeability

layer is 3 times faster flowing. After a second microcapsule treatment, followed by 9 pore volumes of water, the high permeability layer remains 3 times faster flowing. This reveals that there is no accumulative effect of flowing micro-capsules and there seems to be a threshold value on the amount of micro-capsules that remain attached to the glass beads after water flushes. It should be noted that, as expected, the experiment with selective microcapsule flow showed a larger overall drop in the relative flow in the two layers.

It would be interesting in the future to see whether this blockage effect is seen for very small micro-capsules, in the sub-micron range. This could show us the extent of the polymer swelling for sub-micron particles in large pore throats. However, the danger with sub-micron particles is the low delivery of active ingredient as the core to shell ratio is extremely small.

4. Conclusion

pH-responsive micro-capsules with a core of hydroxypropyl cellulose and a shell of poly(4-vinyl pyridine), made using a solvent precipitation method, have been shown to preferentially block high permeability regions of a porous medium. The micro-capsules, of sizes 2 – 7 μm in diameter have a tendency to be retained in the matrix of the pack made of 0.5 and 1.0 mm glass beads. The swelling of the micro-capsule shell during acidification constricted the pore throats of the low permeability layer much more than the high permeability layer.

There seems to be a threshold value for the amount of micro-capsules that can be retained in the glass beads matrix after successive water flushes. Selective micro-capsule flowing produced a larger drop in the relative flow speed in between the high and low permeability layers. The

release of hydroxypropyl cellulose during acidification was sufficient to continue blocking the pack to the same extent.

The size of the microcapsules needed is governed by the pore throat sizes of the oil reservoirs. With sandstone reservoirs, the higher pore throat sizes would indicate the need for larger micro-capsules to see the blockage effect from these micro-capsules. More information is required to get vital information about the pore throats of each individual reservoir before allowing such treatment to avoid plugging the reservoir with the wrong micro-capsule size.

Acknowledgements

The authors are very grateful to Ian Collins, Brian Gane, Harry Frampton and Dave Chappell from BP for helpful advice. Financial support from BP and Mr. Yousef Jameel is gratefully acknowledged.

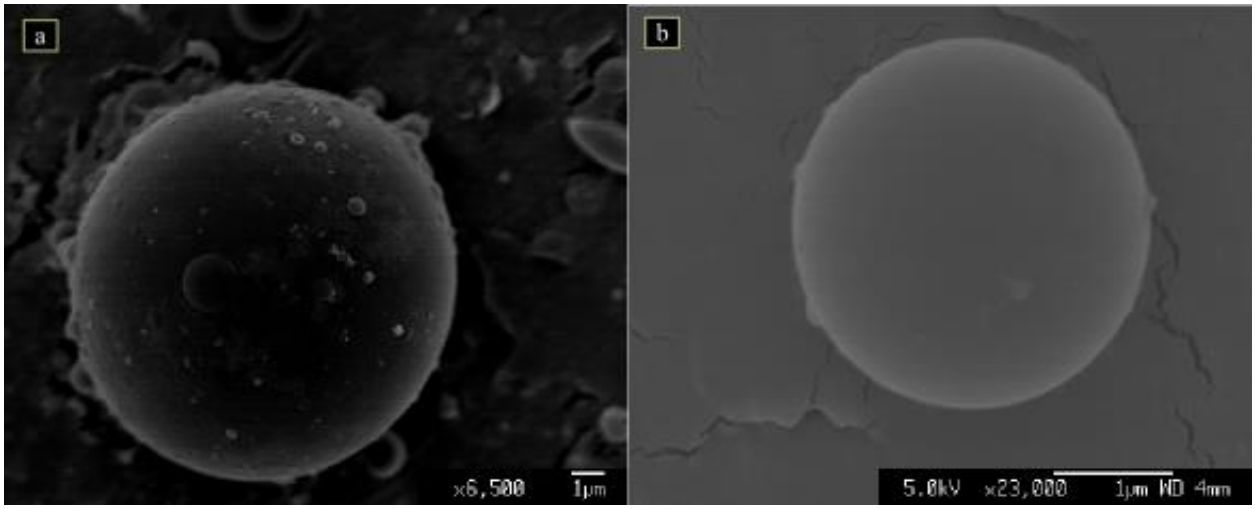

Figure 1: Scanning Electron Microscope (SEM) images of Poly(lactic-co-glycolic) shell micro-capsules with hydroxypropyl cellulose in the core (Gun and Routh, 2013a).

Figure 2: Photo of the flow tank with dual permeability layers in parallel and another layer in series (note the metal mesh included in the middle of high permeability layer).

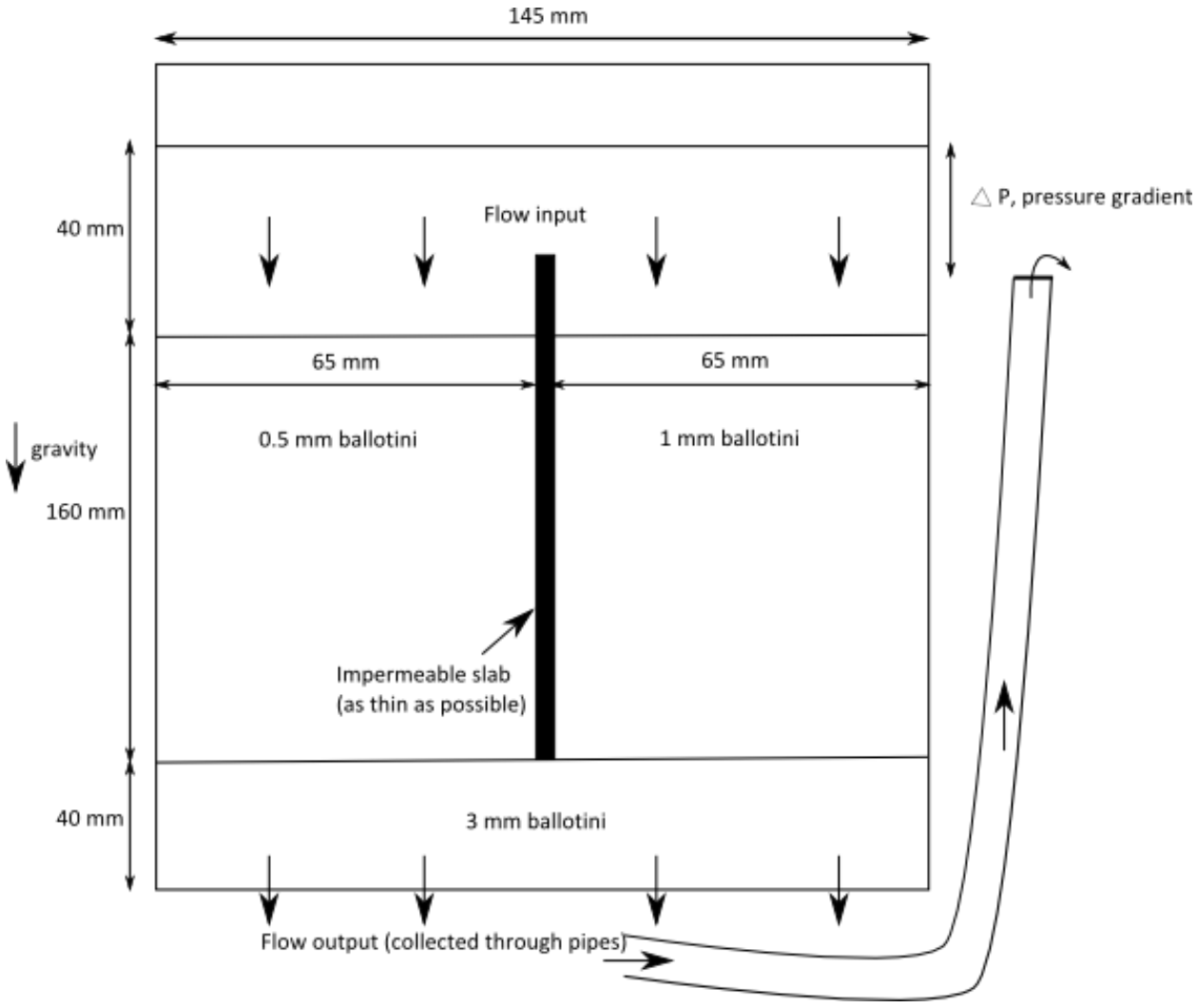

Figure 3: Schematic of the flow tank, showing the different permeability regions (not to scale).

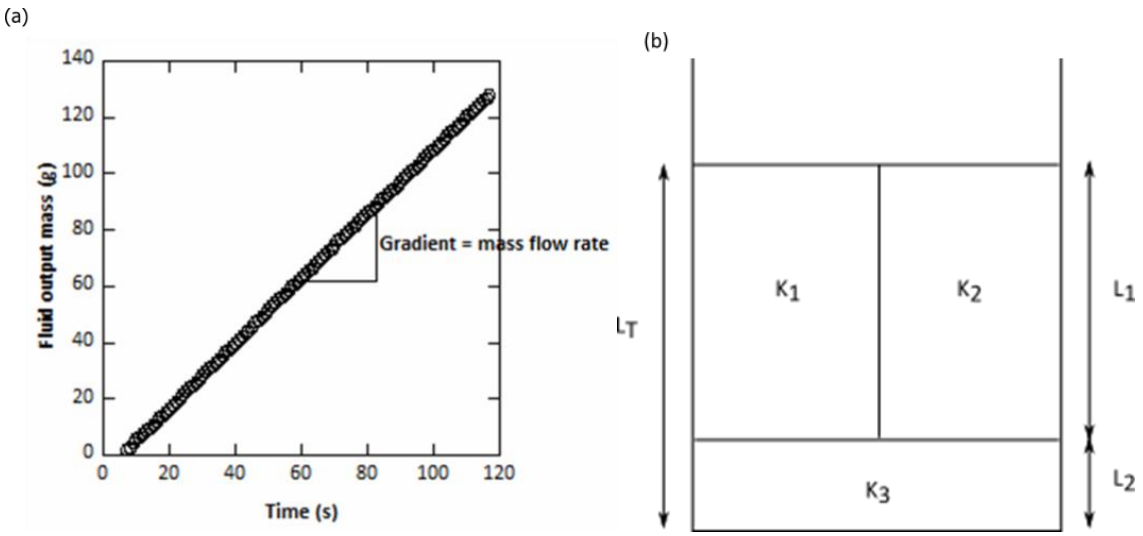

Figure 4:(a) Typical graph of fluid flow against time from the data-logged weighing scale. (b) Schematic of permeability layers in parallel and series.

(a)

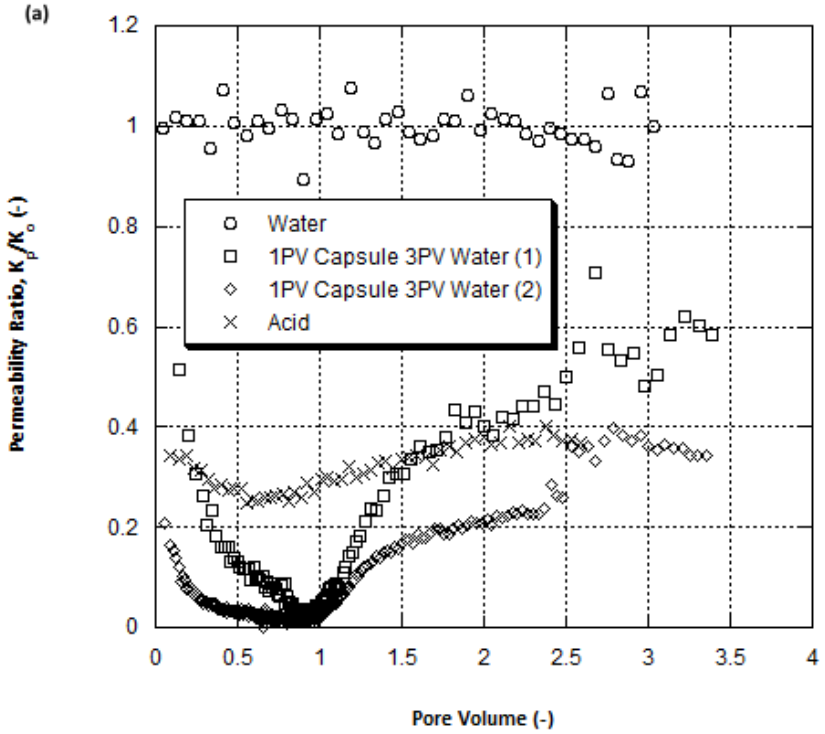
Permeability Ratio, K_p/K_o (-)
Pore Volume (-)
Water
1PV Capsule 3PV Water (1)
1PV Capsule 3PV Water (2)
Acid
0
0.2
0.4
0.6
0.8
1
1.2
0.5
1.5
2
2.5
3
3.5
4

(b)

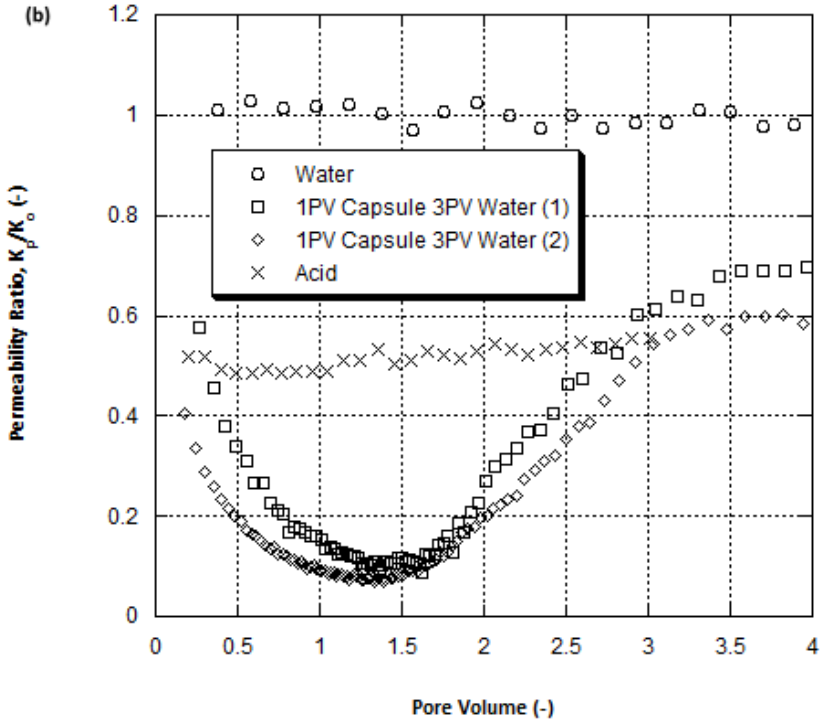
Permeability Ratio, K_p/K_o (-)
Pore Volume (-)
Water
1PV Capsule 3PV Water (1)
1PV Capsule 3PV Water (2)
Acid
0
0.2
0.4
0.6
0.8
1
1.2
0.5
1.5
2
2.5
3
3.5
4

Figure 5: Graph of permeability ratio against pore volume for single permeability layer experiments (1.0 mm diameter glass beads) (a) With HPC in the micro-capsule core (b) Without HPC in the micro-capsule core.

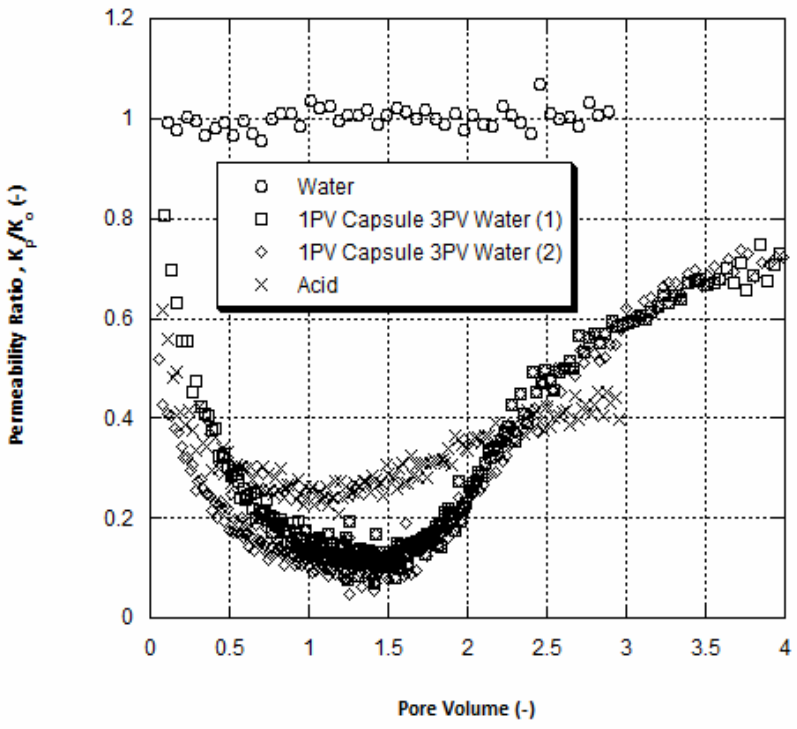
Permeability Ratio , K_p/K_o (-)
Pore Volume (-)
Water
1PV Capsule 3PV Water (1)
1PV Capsule 3PV Water (2)
Acid
0
0.2
0.4
0.6
0.8
1
1.2
0
0.5
1
1.5
2
2.5
3
3.5
4

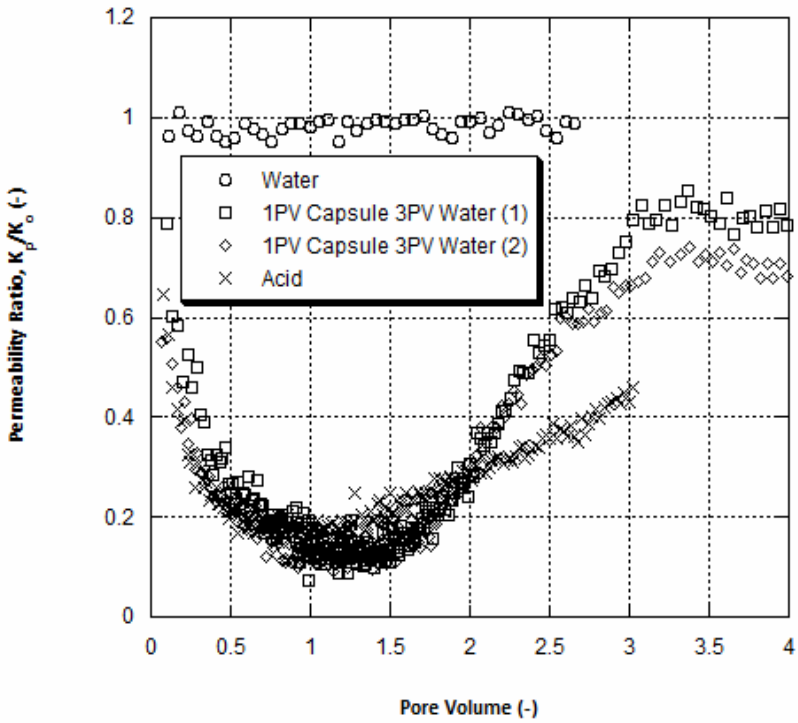
Permeability Ratio, K_p/K_o (-)
Pore Volume (-)
Water
1PV Capsule 3PV Water (1)
1PV Capsule 3PV Water (2)
Acid
0
0.2
0.4
0.6
0.8
1
1.2
0
0.5
1
1.5
2
2.5
3
3.5
4

Figure 6: Graph of permeability ratio against pore volume for single low permeability layer experiments (0.5 mm diameter glass beads) (a) With HPC in the micro-capsule core (b) Without HPC in the micro-capsule core.

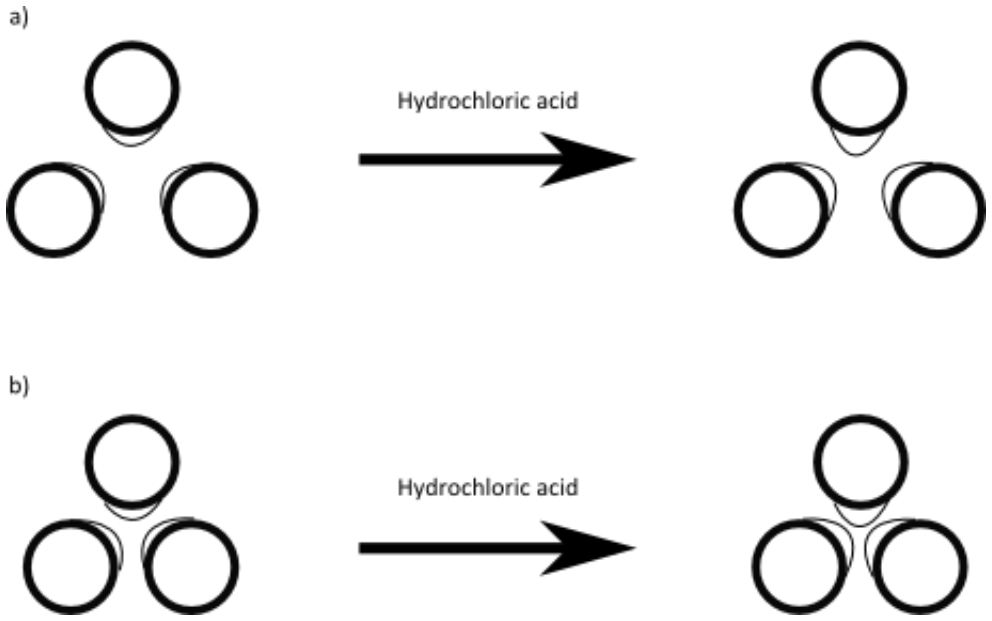

Figure 7: Schematic of the pore throats before and after hydrochloric acid flow (a) High permeability layer (1.0 mm diameter glass beads) (b) Low permeability layer (0.5 mm diameter glass beads).

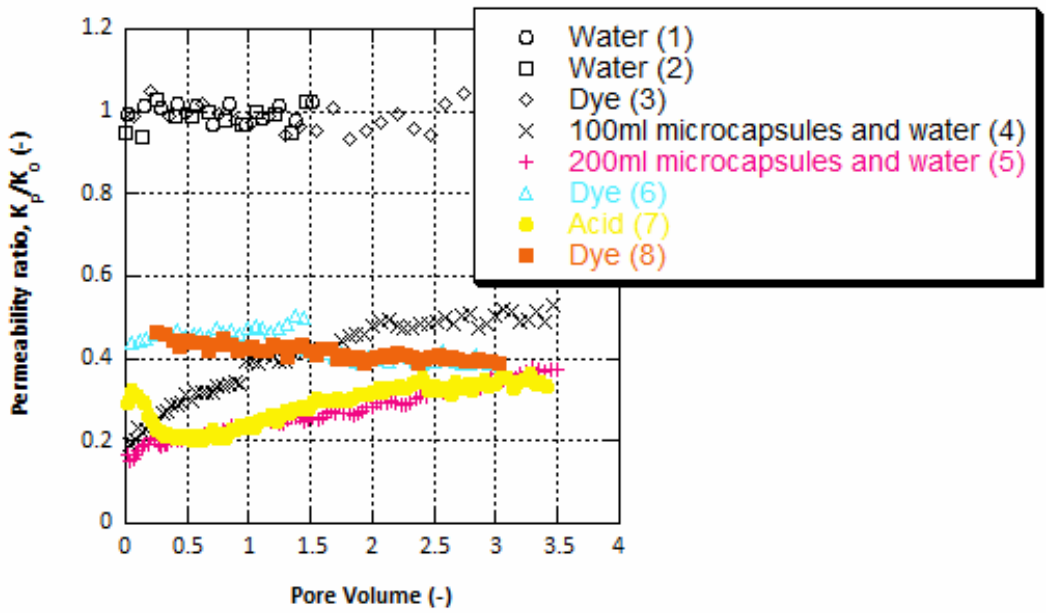

Figure 8: Graph of permeability ratio against pore volume for dual permeability layer experiment where the micro-capsule dispersion was selectively flowed into the high permeability layer (1.0 mm diameter glass beads).

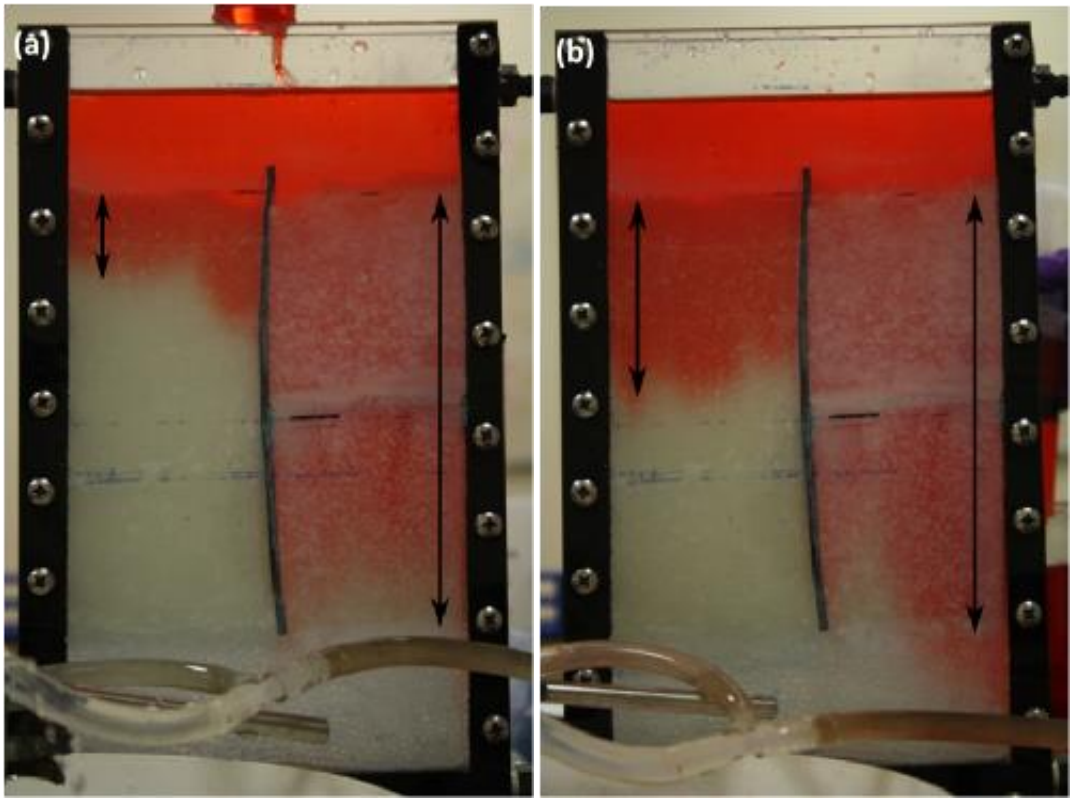

Figure 9: Flow front pictures of dual permeability tank experiments with selective micro-capsule flow (a) Before micro-capsules (b) After 200 mL micro-capsules and three and a half pore volumes of deionised water. High permeability on the right side, low permeability on the left.

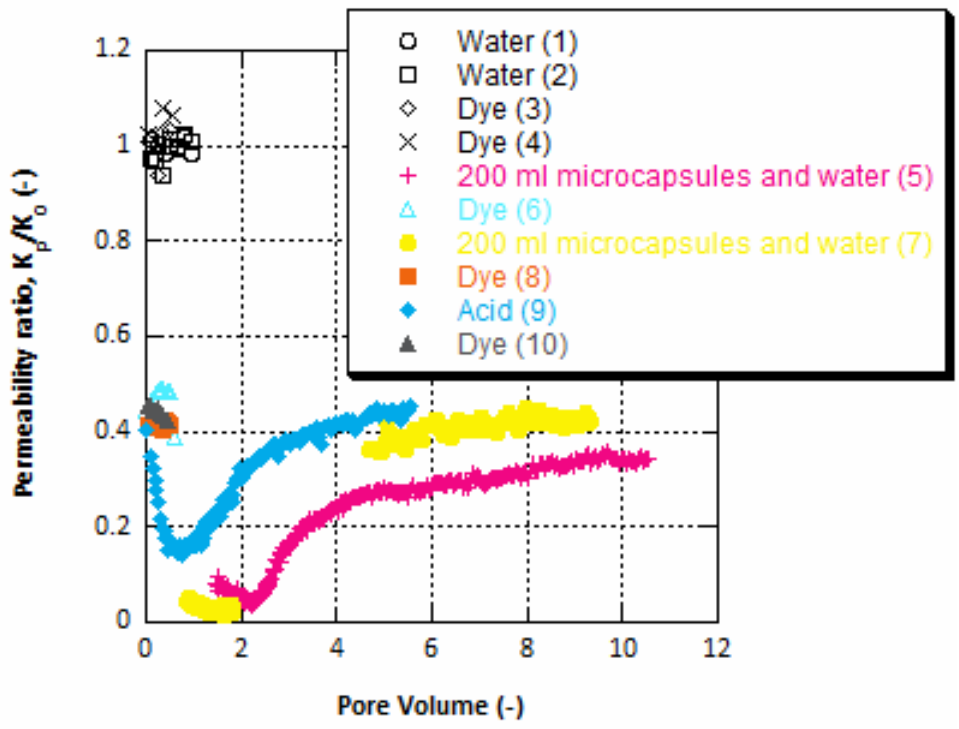

Figure 10: Graph of permeability ratio against pore volume for dual permeability layer experiment where the micro-capsule dispersion was allowed to freely flow through both the high and low permeability layers.

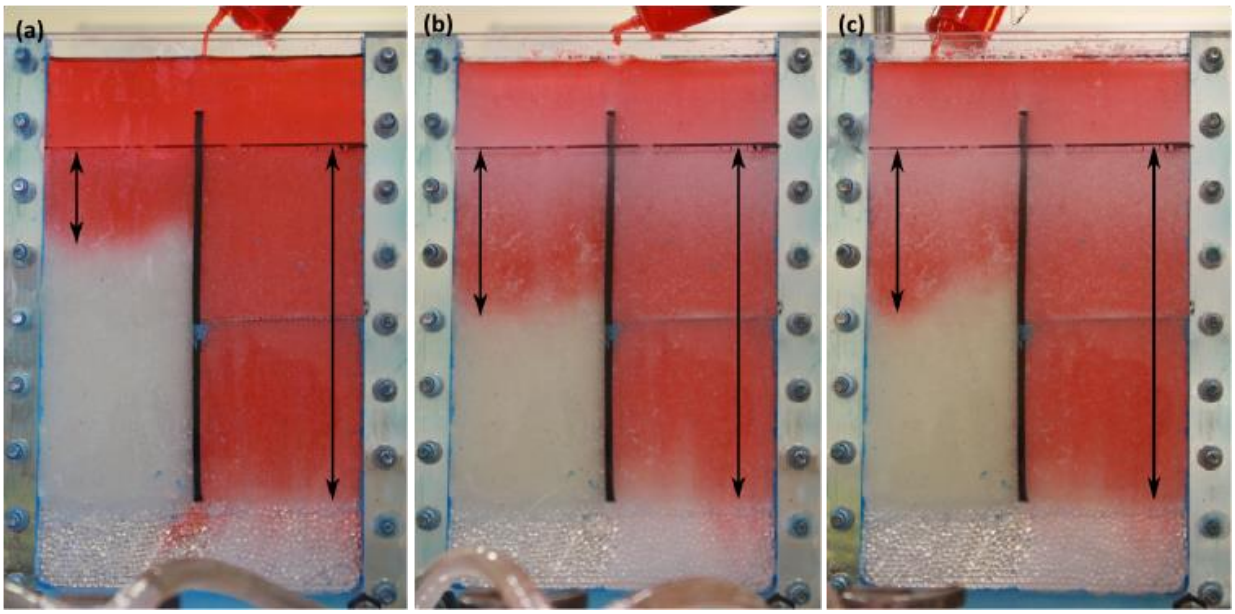

Figure 11: Flow front pictures of dual permeability tank experiments with non-selective micro-capsule flow (a) Before micro-capsules (b) After 200 mL micro-capsules and ten pore volumes of deionised water (c) After another 200 mL micro-capsules and nine pore volumes of deionised water. High permeability on the right side, low permeability on the left.

Table 1: Comparison between predicted and measured flow rates of the tank.

Pressure difference (Pa)	**Predicted flow rate using equation 1 (10^{-6} m^3 s^{-1})**	**Measured flow rate (10^{-6} m^3 s^{-1})**		**% Difference between measured and predicted values**	
		Experiment 1	**Experiment 2**	**Experiment 1**	**Experiment 2**
402	1.51	1.50	1.49	0.51	1.19
1226	4.62	4.33	4.28	6.28	7.36
2492	9.38	8.25	8.13	12.0	13.3

References:

Avery, R., Ramsay, J., 1973. **The sorption of nitrogen in porous compacts of silica and zirconia powders.** Journal of Colloid and Interface Science (1973), p. 42

Bertkau, W., Steidl, N., Se, B., 2012. Patent US20120222863 - **Alkanesulfonic acid microcapsules and use thereof in deep wells**

Chwang, A.B., Rothman, M.A., Mao, S.Y., Hewitt, R.H., Weaver, M.S., Silvernail, J.A., Rajan, K., Hack, M., Brown, J.J., Chu, X., Moro, L., Krajewski, T., Rutherford, N., 2003. **Thin film encapsulated flexible organic electroluminescent displays.**Applied Physics Letters 83 (2003), p. 413

Ciftcioglu, M., Smith, D.M., Ross, S.B., 1988. **Mercury porosimetry of ordered sphere compacts: Investigation of intrusion and extrusion pore size distributions.** Powder Technology 55 (1988), pp. 193–205

Gun, W.J., Routh, A.F., 2013a. **Formation and characterisation of pH-responsive liquid core microcapsules.** Langmuir (2013)

Gun, W.J., Routh, A.F., 2013b. **Microcapsule flow in porous media.** Chemical Engineering Science 102 (2013), pp. 309–314

Keen, P.H.R., Slater, N.K.H., Routh, A.F., 2012. **Encapsulation of lactic acid bacteria in colloidosomes.** Langmuir28 (2012), pp. 16007–16014

Kruyer, S., 1958. **The penetration of mercury and capillary condensation in packed spheres.** Transactions of the Faraday Society 54 **(**1958), pp. 1758–1767

Montanaro, L., 2012. Patent WO2012090158A1 - **Method for recovering oil from a reservoir by means of micro (nano) - structured fluids with controlled release of barrier substances**

Moody, L.F., 1944. **Friction factors for pipe flow.** Trans. Asme 66 (1944), pp. 671–684

Nasseau, M., Boublik, Y., Meier, W., Winterhalter, M., Fournier, D., 2001. **Substrate-permeable encapsulation of enzymes maintains effective activity, stabilizes against denaturation, and protects against proteolytic degradation.** Biotechnology and bioengineering 75 (2001), pp. 615–618

Samuel, M., Sengul, M., 2003. **MEARR Number 4, Schlumberger.** Middle East and Asia Reservoir Review (MEARR) 4

Seo, S.-W., Chae, H., Joon Seo, S., Kyoon Chung, H., Min Cho, S., 2013. **Extremely bendable thin-film encapsulation of organic light-emitting diodes.** Applied Physics Letters 102 (2013), 161908

Sinnott, R. K., Coulson and Richardson's Chemical Engineering Volume 6: Chemical Engineering Design, 4th Edition, Elsevier, 2005

Tachaprutinun, A., Udomsup, T., Luadthong, C., Wanichwecharungruang, S., 2009. **Preventing the thermal degradation of astaxanthin through nanoencapsulation.** International journal of pharmaceutics 374 (2009), pp. 119–124

Tchelepi, H.A., Orr, F.M., N. Rakotomalala, D. Salin, R. Wouméni, 1993.**Dispersion, permeability heterogeneity, and viscous fingering: acoustic experimental observations and particle-tracking simulations.** Physics of Fluids A: Fluid Dynamics, 5 (1993), p.1558